

**SANDIA REPORT**

SAND97-2325 • UC-706  
Unlimited Release  
Printed September 1997

RECEIVED  
OCT 06 1997  
O.S.T.I.

# **General Application of Rapid 3-D Digitizing and Tool Path Generation for Complex Shapes**

DISTRIBUTION OF THIS DOCUMENT IS UNLIMITED

Kwan S. Kwok, Clifford S. Loucks, Brian J. Driessen

MASTER

Prepared by  
Sandia National Laboratories  
Albuquerque, New Mexico 87185 and Livermore, California 94550

Sandia is a multiprogram laboratory operated by Sandia Corporation,  
a Lockheed Martin Company, for the United States Department of  
Energy under Contract DE-AC04-94AL85000.

Approved for public release; distribution is unlimited.



**Sandia National Laboratories**

Issued by Sandia National Laboratories, operated for the United States Department of Energy by Sandia Corporation.

**NOTICE:** This report was prepared as an account of work sponsored by an agency of the United States Government. Neither the United States Government nor any agency thereof, nor any of their employees, nor any of their contractors, subcontractors, or their employees, makes any warranty, express or implied, or assumes any legal liability or responsibility for the accuracy, completeness, or usefulness of any information, apparatus, product, or process disclosed, or represents that its use would not infringe privately owned rights. Reference herein to any specific commercial product, process, or service by trade name, trademark, manufacturer, or otherwise, does not necessarily constitute or imply its endorsement, recommendation, or favoring by the United States Government, any agency thereof, or any of their contractors or subcontractors. The views and opinions expressed herein do not necessarily state or reflect those of the United States Government, any agency thereof, or any of their contractors.

Printed in the United States of America. This report has been reproduced directly from the best available copy.

Available to DOE and DOE contractors from  
Office of Scientific and Technical Information  
P.O. Box 62  
Oak Ridge, TN 37831

Prices available from (615) 576-8401, FTS 626-8401

Available to the public from  
National Technical Information Service  
U.S. Department of Commerce  
5285 Port Royal Rd  
Springfield, VA 22161

NTIS price codes  
Printed copy: A03  
Microfiche copy: A01

# **General Application of Rapid 3-D Digitizing and Tool Path Generation for Complex Shapes**

Kwan S. Kwok  
Intelligent System Sensors and Controls Department

Clifford S. Loucks  
Intelligent Systems Department

Brian J. Driessen  
Structural Dynamics Department

Sandia National Laboratories  
P.O. Box 5800  
Albuquerque, NM 87185-1003

## **Abstract**

A system for automatic tool path generation was developed at Sandia National Laboratories for finish machining operations. The system consists of a commercially available 5-axis milling machine controlled by Sandia developed software. This system was used to remove overspray on cast turbine blades. A laser-based, structured-light sensor, mounted on a tool holder, is used to collect 3D data points around the surface of the turbine blade. Using the digitized model of the blade, a tool path is generated which will drive a 0.375" CBN grinding pin around the tip of the blade. A fuzzified digital filter was developed to properly eliminate false sensor readings caused by burrs, holes and overspray. The digital filter was found to successfully generate the correct tool path for a blade with intentionally scanned holes and defects. The fuzzified filter improved the computation efficiency by a factor of 25. For application to general parts, an adaptive scanning algorithm was developed and presented with simulation and experimental results. A right pyramid and an ellipsoid were scanned successfully with the adaptive algorithm in simulation studies. In actual experiments, a nose cone and a turbine blade were successfully scanned. A complex shaped turbine blade was successfully scanned and finish machined using these algorithms.

## **Acknowledgment**

This project was a team effort, and the authors wish to thank the rest of the team. Colin B. Selleck was the principal researcher on the structured light system. Larry P. Ray developed the bi-cubic spline algorithms specific for this research and performed the calibration of structured lighting to the CNC machine. Greg Starr performed the kinematic analysis of the Fadal CNC Vertical Machining Center. The authors also wish to thank Perry A. Molley who was the manager at the time this work was done.

## **DISCLAIMER**

**Portions of this document may be illegible  
in electronic image products. Images are  
produced from the best available original  
document.**

## Table of Contents

<b>Introduction .....</b>	<b>7</b>
<b>Statement of the Problem.....</b>	<b>8</b>
<b>Tool Path Generation Method .....</b>	<b>8</b>
<b>Digital Filtering .....</b>	<b>11</b>
<b>Adaptive Scanning Algorithm.....</b>	<b>12</b>
<b>Results .....</b>	<b>14</b>
<b>Conclusion.....</b>	<b>20</b>
<b>References.....</b>	<b>20</b>
<b>Appendix A.....</b>	<b>21</b>

## Table of Figures

<b>Figure 1 Design Vs Actual Blades.....</b>	<b>9</b>
<b>Figure 2 Laser-based Structured Light-Sensor Setup.....</b>	<b>9</b>
<b>Figure 3 Generated Tool Path.....</b>	<b>10</b>
<b>Figure 4 Tilt-angle of the Blade during Machining.....</b>	<b>10</b>
<b>Figure 5 Schematic Illustrating Sensor Notation.....</b>	<b>13</b>
<b>Figure 6 Result of Fuzzified Lowess Filter Applied to a Scanned Hole.....</b>	<b>15</b>
<b>Figure 7 Comparison of Tool Path Generated with and without the Fuzzified Lowess Filter.....</b>	<b>15</b>
<b>Figure 8 Tilt-angles of the Generated Tool Path.....</b>	<b>16</b>
<b>Figure 9 Simulated Scanner Path, Case of a Right Pyramid.....</b>	<b>16</b>
<b>Figure 10 Projection onto x-y Plane of a Constant-z Portion of Scanner Path of an Ellipsoid.....</b>	<b>17</b>
<b>Figure 11 Path of Point B, in Part Coordinates, Actual Nose Cone Scan.....</b>	<b>17</b>
<b>Figure 12 Path of Point D, in Part Coordinates, Actual Nose Cone Scan.....</b>	<b>18</b>
<b>Figure 13 Path of Point B, in Part Coordinates, Actual Turbine Blade Scan.....</b>	<b>18</b>
<b>Figure 14 Path of Point D, in Part Coordinates, Actual Turbine Blade Scan.....</b>	<b>19</b>
<b>Figure 15 Path of Point B, in Part Coordinates, Blow-up of Corner Detection/Navigation, Actual Turbine Blade Scan.....</b>	<b>19</b>

# General Application of Rapid 3-D Digitizing and Tool Path Generation for Complex Shapes

## Introduction

There are many applications where machining and finishing operations are required on complex surfaces. The fabrication of stamping dies, for example, is an iterative process where the initial die shape is first defined in a CAD system. Tool paths are then computed and the shape is created with a CNC machining center. Initial stampings reveal areas where the shape must be changed either by removing existing material or adding material where it is deficient. These finishing operations are performed manually today by a skilled craftsman because no system exists which can measure the error in the stamping and automatically define the process parameters to adjust the shape of the die.

Manufacturing machines are traditionally designed for large volume production capabilities and are time consuming and tedious to retool for different tasks. Production machines that are easily reprogrammed, heuristic by design, intelligent, and highly adaptable for a variety of manufacturing tasks are needed in the agile manufacturing technologies area. The emphases on these machines are the flexibility and ability to make rapid design and product changes based on market demands. Sandia has developed robotics and automation techniques that make use of sensors, CAD information, and intelligent algorithms to improve manufacturing processes. Consequently, we applied fuzzy logic techniques to the tool path generation processing in this research. Specifically we have employed fuzzy selection criteria in processing the data collected by the structured light sensor, and in the scan step-size selection of the adaptive scanning algorithm.

Zadeh [1] introduced fuzzy logic to describe systems that are “too complex or too ill-defined to admit of precise mathematical analysis.” Its major features are the use of linguistic rather than numerical variables and the characterization of relations between variables by “fuzzy” conditional statements. Mamdani and Assilian [2], recognizing that fuzzy logic provided a means of dealing with uncertainty, extended the concept to industrial process control in the expectation that it would be applied to systems for which precise measurements of the state variables could not be obtained. Processes to which the fuzzy, rule-based approach has been applied include cement kilns, wood pulp grinders, and sewage treatment plants [3]. Fuzzy logic was used in this research for data smoothing and in the adaptive algorithm for intelligent scanning of unknown parts.

This report describes research conducted in the Intelligent Systems and Robotics Center (ISRC) of Sandia National Laboratories (SNL) to further develop sensor-directed, automated surface and edge finishing operations on cast and machined parts. As an example application, this technology was applied to Sprayed Abrasive Tip (SAT) overspray removal on cast turbine blades.

## Statement of the Problem

Many manufacturing operations utilize processes such as investment casting to fabricate metal parts with complex shapes. Alternate fabrication techniques, such as machining, are either incapable of forming the required shapes or require too much effort, resulting in prohibitively expensive parts. Due to dimensional variations inherent with the casting process, cast parts typically require additional machining operations to create precision features. Since current automated machining technology is based on precise position knowledge of the part to be machined, automation on cast parts is frequently impossible because of the dimensional uncertainties resulting from the casting process.

Just as the piston rings improve compression and efficiency in automobile engines, one measure of combustion efficiency in jet engines is how small the gap between the tips of the turbine blades and the inside of the engine case (shroud) can be made. Too big a gap results in leakage, too small a gap and differential thermal expansion (as the engine operating conditions are changed) could drive the blades directly into the shroud. The latter is actually preferred if the blades are designed to handle the interference and grind out the inside of the shroud. This is exactly what's being done with the Sprayed Abrasive Tip blades in the jet engine manufacturing industry.

After the blades are formed by investment casting, a silicon carbide grit is applied to the tips of the blades and bonded in place by plasma spraying a nickel alloy which extends the metal matrix of the blades up around the grit. The plasma spraying operation, however, leaves excess material extending 0.05" to 0.10" down the sides of the blades. This excess material must be ground off to recreate the blade's airfoil shape, a process that must be tightly controlled both for the aerodynamic efficiency of the airfoil as well as ensuring there are no disjoint surfaces (stress risers) which would lead to failure when the blade is subjected to the high-temperature, high-stress environment of an operating jet engine.

While grinding the overspray off the complex contours of the blade tips to less than 0.001" tolerance is difficult enough, it's made impossible for conventional CNC machines since, as castings, each blade is unique. Investment casting can produce intricate shapes, such as the cooling passages inside these hollow blades, but cannot yield identical parts. During solidification, the blades tend to shrink and warp, producing variances of  $\pm 0.030"$  in the location of the tip from blade to blade. Consequently, a unique tool path to grind off the overspray is needed for each blade. Figure 1 illustrates typical variations among the design blade and two actual blades.

## Tool Path Generation Method

A system capable of grinding the overspray off the blades has been developed. The system is an integration of commercially available equipment, controlled by Sandia developed software. To process a blade, the blade is fixtured in a 5-axis milling machine.

A laser-based, structured-light sensor, mounted on a tool holder, is used to collect 3D data points around the surface of the blade tip, adjacent to the overspray.

### Design vs Actual Blades

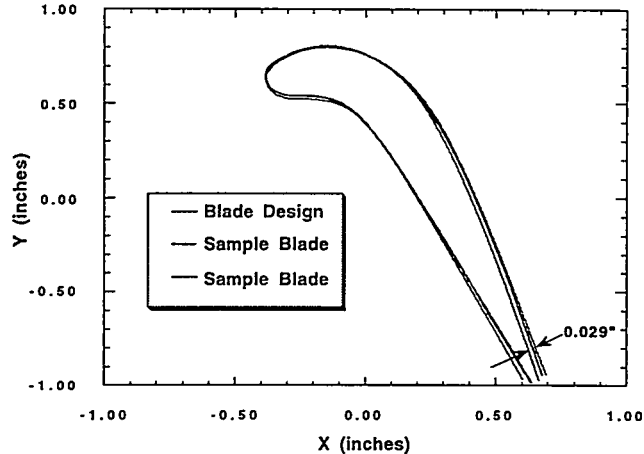


**Figure 1 Design Vs Actual Blades.**

Figure 2 shows a schematic diagram of the structured light system setup. Based on tensor product surfaces, the data points are analyzed to produce a CAD file in the format of cross-sections at various heights along the blade. Typically, 4 bicubic splines are used to describe each cross-section. Using this digitized model of the blade, a tool path is generated which will drive a 0.375" Cubic Boron Nitride (CBN) grinding pin around the tip of the blade.

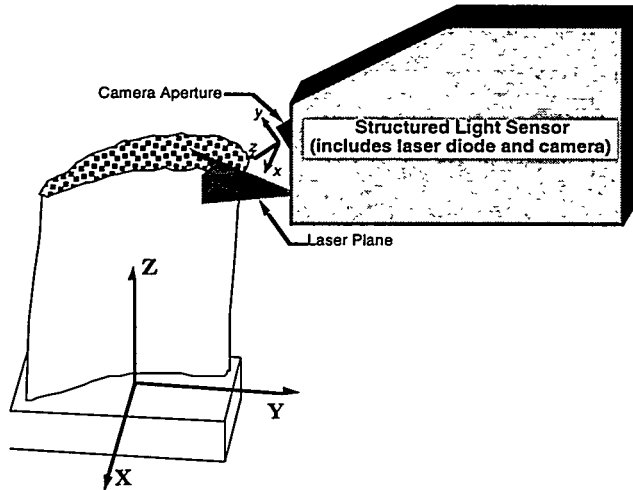


**Figure 2 Laser-based Structured Light-Sensor Setup.**

Figure 3 shows the generated tool path, and Figure 4 shows the tilt-angle, Alpha, of the blade for the machining operation based on the design blade. A low-pass filter is deployed for the smoothing performed on the tilt-angles in Figure 4.

### Tool Path from Design Data

computed same way as with digitized data

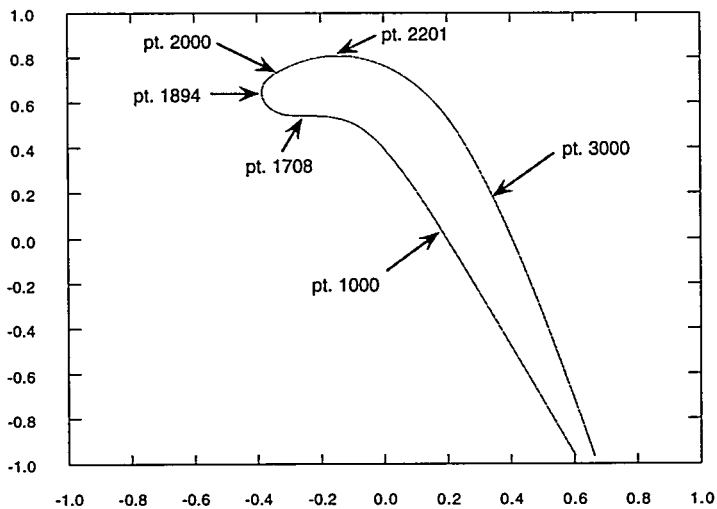


Figure 3 Generated Tool Path.

This path is downloaded to the milling machine, which now holds a high speed spindle and the grinding pin as a tool, and the overspray is removed in a one-pass, creep-feed grinding operation. In preliminary tests, the overspray was completely removed from a test blade leaving a mismatch of less than 0.001".

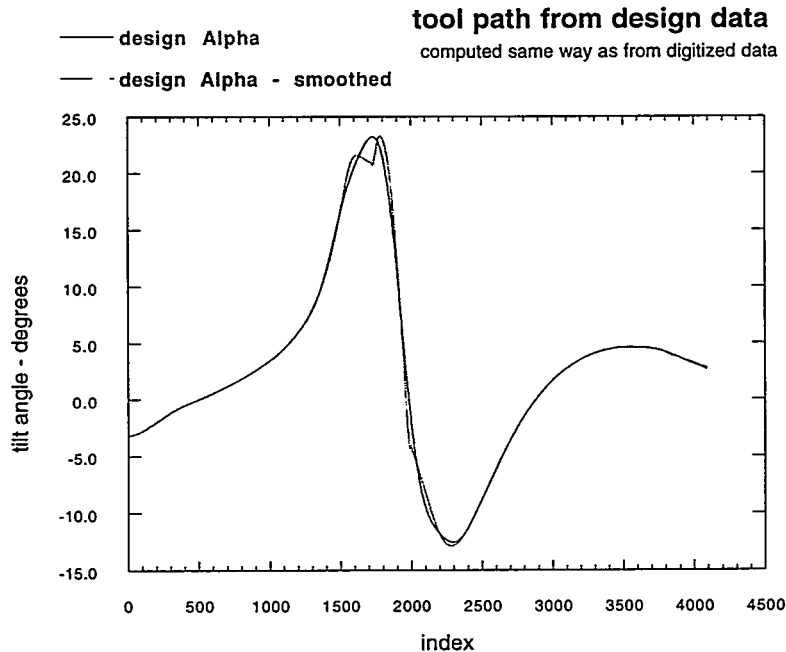


Figure 4 Tilt-angle of the Blade during Machining.

## Digital Filtering

The tool path generation method described above works for most blades that have smooth finishes with relatively few flaws and defects on the surface where the scan plane lies. However, when the scan surface contains burrs, holes or overspray, the structured light sensor would mistakenly average the burr, hole or overspray to the actual surface and would, therefore, produce an incorrect profile to be used in generating the tool path. This would render the blade to be unacceptable following the finishing operation. A digital filter was developed to avoid this problem.

The digital filter developed for this application is a fuzzified lowess (locally-weighted scatterplot smoother) filter [4][5]. The fuzzified parameter is the smoothness parameter  $f$ , which is a number between 0 and 1. As  $f$  increases, the smooth curve becomes smoother, but computational requirements increase exponentially. The goal is to choose  $f$  to be as large as possible to get as much smoothness as possible without distorting the underlying pattern in the data, and not too large so that the computations can be completed within a reasonable time. Fuzzy rules are used in choosing the  $f$  value during execution. If the scanned curvature of the surface is large,  $f$  is chosen to be small. If the curvature is small,  $f$  is chosen to be large [5]. Fuzzy logic is an ideal choice for solving this kind of optimization problem.

In the lowess procedure, the program first chooses  $f$ , which is approximately the fraction of points to be used in the computation of each fitted value. First, let  $q$  be  $fn$  rounded to the nearest integer, where  $n$  is the number of data points to be smoothed. Second, let  $d_i$  be the distance from  $x_i$  to its  $q$ th nearest neighbor along the  $x$  axis. ( $x_i$  is counted as a neighbor of itself.) Let  $T(u)$  be the tricubic weight function:

$$T(u) = \begin{cases} (1 - |u|^3)^3 & \text{for } |u| < 1 \\ 0 & \text{otherwise} \end{cases}$$

Then the weight given to the point  $(x_k, y_k)$  when computing a smoothed value at  $x_i$  is defined to be

$$t_i(x_k) = T\left[\frac{x_i - x_k}{d_i}\right]$$

To compute a fitted value at  $x_i$  in the first stage of lowess, a line (or constant if  $d_i = 0$ ) is fitted to the points of the scatter plot using weighted least squares with weight  $t_i(x_k)$  at the point  $(x_k, y_k)$ . That is, values of  $a$  and  $b$  are found which minimize

$$\sum_{k=1}^n t_i(x_k) (y_k - a - b x_k)^2$$

If  $\hat{a}$  and  $\hat{b}$  are the values that achieve the minimum, then the initial fitted value at  $x_i$  is defined to be

$$\hat{y}_i = \hat{a} + \hat{b}x_i$$

Following the computation of initial fitted values for all  $x_i$ , residuals are computed,

$$r_i = y_i - \hat{y}_i$$

and robustness weights are computed from them. Let  $B(u)$  be the bisquare weight function:

$$B(u) = \begin{cases} (1 - |u|^2)^2 & \text{for } |u| < 1 \\ 0 & \text{otherwise} \end{cases}$$

Let  $m$  be the median of the absolute values of the residuals, that is,

$$m = \text{median}|r_k|$$

The robustness weight for the point  $(x_k, y_k)$  is defined to be

$$w(x_k) = B\left[\frac{r_k}{6m}\right]$$

The median absolute residual,  $m$ , is a measure of how spread out the residuals are. If a residual is small compared with  $6m$ , the corresponding robustness weight will be close to 1. If a residual is greater than  $6m$ , the corresponding weight is 0.

The next stage is to get updated fitted values, by fitting the line again, but this time incorporating the robustness weights. In the weighted linear regression for refitting  $\hat{y}_i$ , the point  $(x_k, y_k)$  is given weight  $w(x_k)t_i(x_k)$ . If  $(x_k, y_k)$  is a peculiar point with a large residual, it will play a small role, or no role at all, in any of the fitted lines in this latter stage of the computation.

## Adaptive Scanning Algorithm

In this section, we present an adaptive scanning algorithm for scanning surfaces that are unknown a priori. Figure 2 contains a schematic of the structured light scanning sensor. It produces an approximately 0.25 inch wide scan line over which about 400 simultaneous  $(x, y, z)$  position readings are taken. It has a 0.2 inch depth of field and a stand-off of 0.5 inches.

Clearly a collision-free scanning method will need the ability to adjust the orientation and position of the scanner with respect to the part whose surface is unknown a priori. The methodology used is as follows:

Let  $x_{sensor}$ ,  $y_{sensor}$ , and  $z_{sensor}$  denote a frame fixed to the structured-light sensor, where  $z_{sensor}$  points along the direction of the laser light (into the scanned object's surface), and  $y_{sensor}$  is in the plane of the planar laser light field with  $y_{sensor}=0$  at the center of the laser light, (and  $x_{sensor}$  perpendicular to this plane). Point B will denote the point located at the center of the depth of field along the  $z_{sensor}$  direction and at  $x_{sensor} = 0$ ,  $y_{sensor} = 0$ . The width of the scan line (in sensor coordinates) was 120/1000".

Point D will denote the point on the object's surface at the center of scan line (i.e., at  $y_{sensor} = 0$ ). Figure 5 below illustrates this notation.

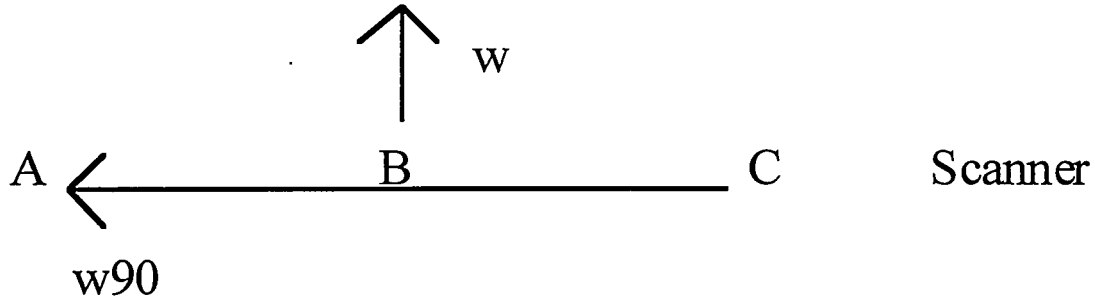


**Figure 5 Schematic Illustrating Sensor Notation.**

Vector  $\bar{n}$  will denote the direction the laser field light is pointing into the object's surface, expressed in part coordinates.

A scan was defined as acceptable if, of all the scan data, the point with smallest  $|y_{sensor}|$  had  $|y_{sensor}|$  less than 0.01" and at least 50 valid data points were obtained along the scan line.

Henceforth, x, y, and z will denote part coordinates of a frame fixed to the part.

We will think of a nose-cone shaped object as a prototype. The z axis points roughly along the axis of the cone. The algorithm scans the surface with B at constant z-values, while keeping the scanner approximately normal to the object's surface. The normal direction is estimated as follows: We fit a straight line in 3-space to the scan line on the object's surface. Since a vector along this line is roughly tangent to the surface, and so is the step direction in the x-y plane, we then take the cross product of these two directions

to obtain an approximate normal to the surface. A constant-z scan is stopped when a revolution of 360 degrees or more has occurred. Then, a step upward, but along the linear fit to the scan line, with its projection onto the last step direction in the x-y plane subtracted out (so that we don't move laterally). The size of this step is chosen so that successive constant-z scan bands are guaranteed to overlap. This procedure is continued until the total distance traveled by point B during a constant-z scan is smaller than some circumference, predetermined so that the top of the cone will be scanned before termination.

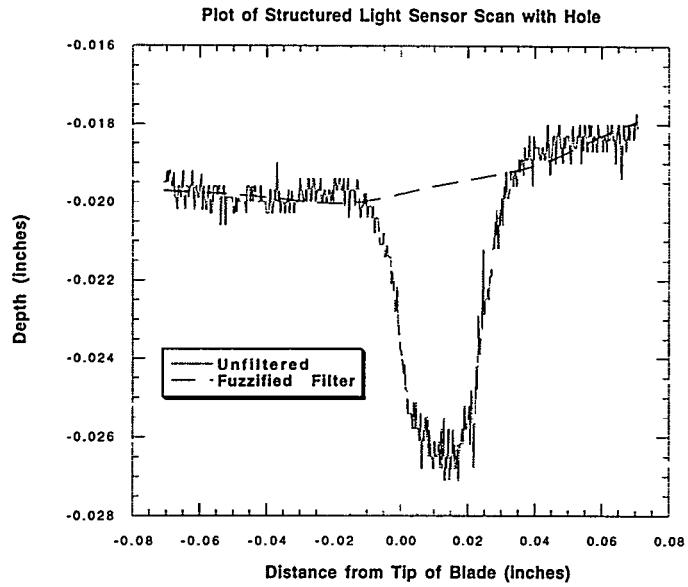
During a constant-z scan, if an unacceptable scan occurs after a step along the step direction denoted herein by  $\bar{v}$  (where  $\bar{v}$  has zero z-component), the step is halved. If a successful scan occurs, the step for the next x-y plane move is doubled, but not to exceed some maximum step length `step_max`. The step length is also potentially reduced by the fuzzy rule set used to adapt step size based on the estimated radius of curvature of the surface. In particular, if  $r$  is small, step length is small; if  $r$  is medium, step length is medium; and if  $r$  is large, step length is large. The membership functions and defuzzification method were chosen so as to make 10 scans occur along a given circumference.

In order to be able to handle objects shaped like pyramids, with sharp edges, a corner detection and navigation loop is included. Clearly if we are moving tangent to the surface and the step size goes to zero (within noise levels), then a corner or edge has been reached. We then rotate  $\bar{n}$  and  $\bar{v}$  about point B, about the z-axis by a fixed incremental value  $\beta$  (10 degrees), step in the v direction, scan, step back along the -v direction, rotate by  $\beta$  again, etc. until the distance between point D (from the scan) and point B increases, indicating that we are now pointing no more than  $\beta^\circ$  past the new tangent direction which follows the corner. Then, normal smooth stepping resumes.

The details of the adaptive scanning algorithm can be found in Appendix A.

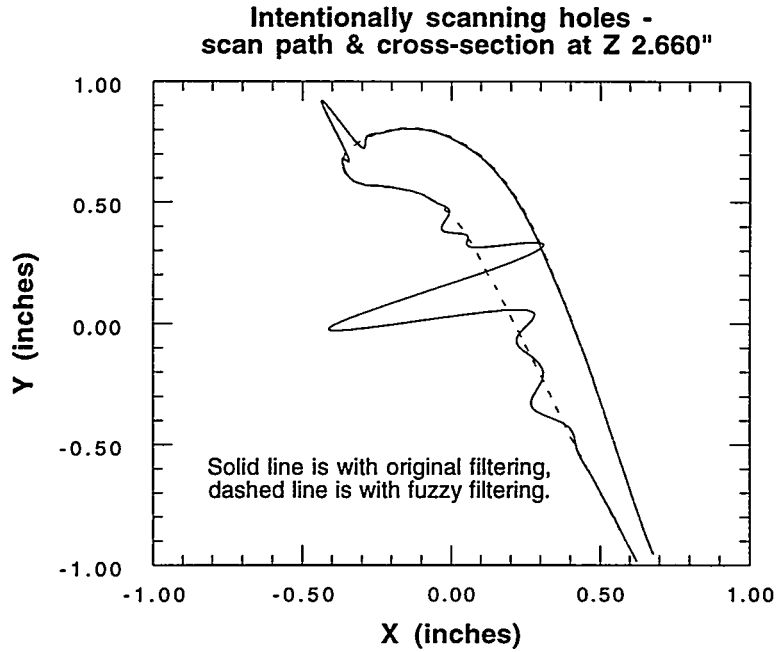
## Results

Results from the generated tool path process without the fuzzified lowess filter produced blades to within 0.001". However, the blade will not pass the manufacturer's requirements without further improvement in the filtering routines for blades with burrs, holes, and overspray. Figure 6 shows the result of using the fuzzified lowess filter on a scanned hole.



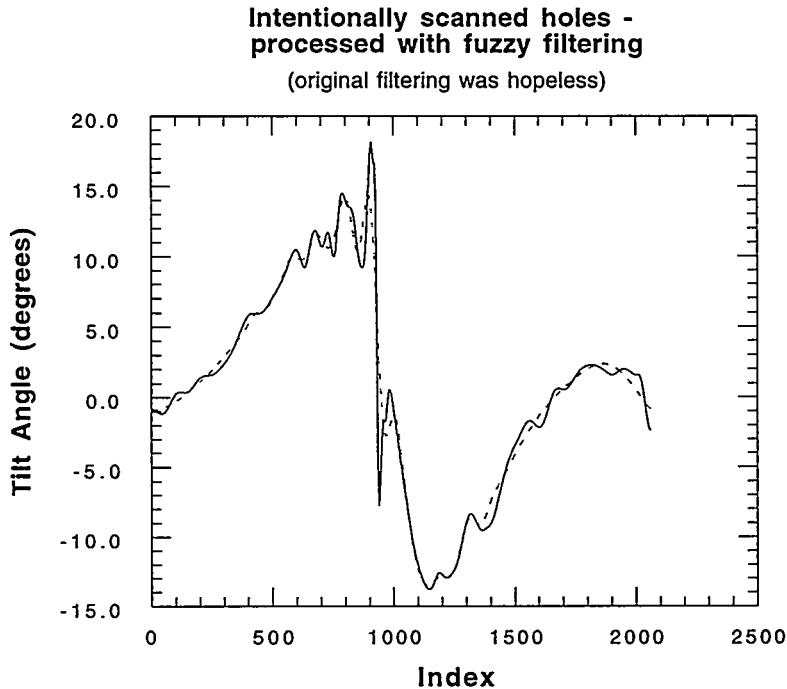
**Figure 6 Result of Fuzzified Lowess Filter Applied to a Scanned Hole.**

The unfiltered structured light output is extremely noisy and the filter successfully located the true surface for the tool path to be generated properly. This can be seen in Figure 7 where the unfiltered tool path is compared with the filtered one. The unfiltered tool path is unusable.



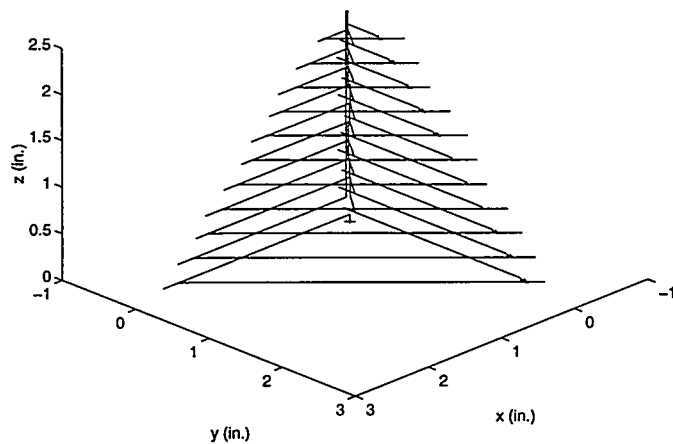
**Figure 7 Comparison of Tool Path Generated with and without the Fuzzified Lowess Filter.**

Figure 8 shows the tilt-angle of the surface normal. It can be seen that the fuzzified lowess filter reduced the oscillation on the surface normal but did not eliminate it completely.



**Figure 8** Tilt-angles of the Generated Tool Path.

In order to extend the automatic tool path generation technology to general parts, the adaptive scanning algorithm was developed. The scanning algorithm was simulated on a right pyramid whose apex is at  $(0,0,2.5")$ . Figure 9 below shows the path of point B for this simulation [5].



**Figure 9** Simulated Scanner Path, Case of a Right Pyramid.

Also, Figure 10 below illustrates a 2D portion of the scan path for the case of an ellipsoid.

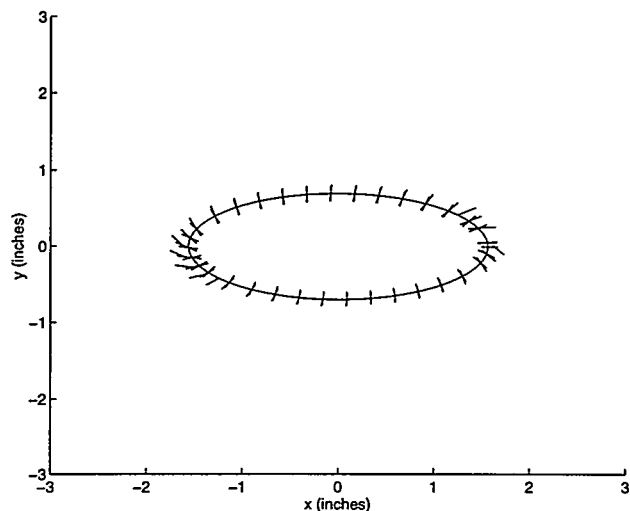


**Figure 10** Projection onto x-y Plane of a Constant-z Portion of Scanner Path of an Ellipsoid.

Experiments were conducted following simulations. A nose cone-shaped object and a turbine blade were scanned in order to demonstrate the adaptive scanning algorithm. The experimental results for the cone-shaped object are shown in Figure 11 and Figure 12, below.

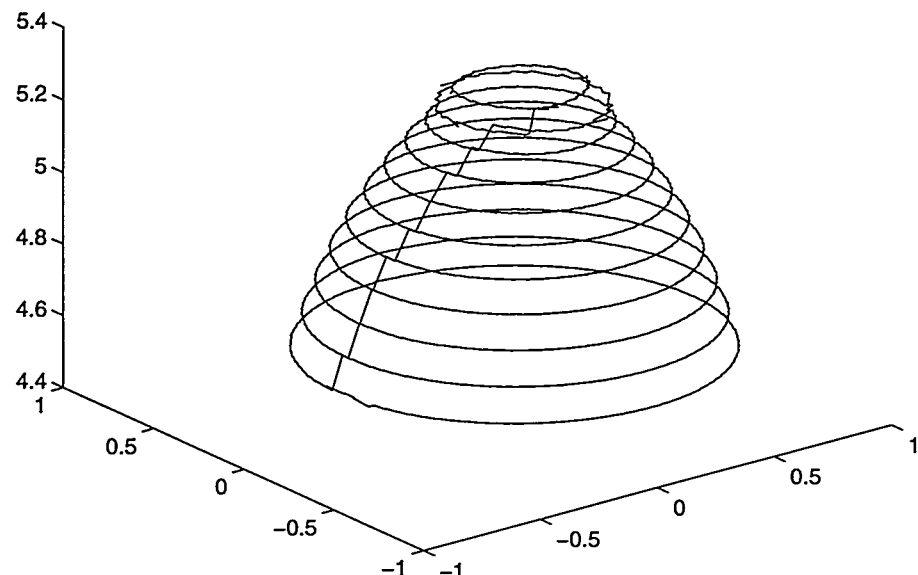


**Figure 11** Path of Point B, in Part Coordinates, Actual Nose Cone Scan.

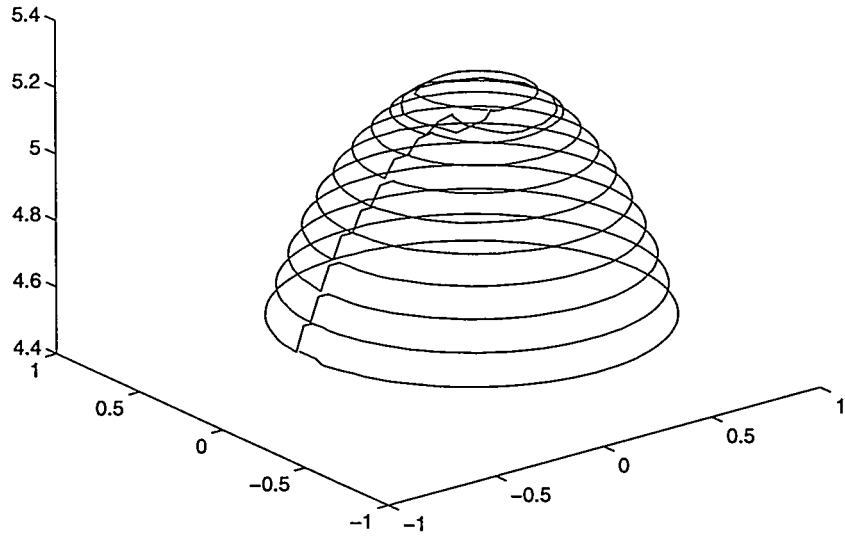


**Figure 12 Path of Point D, in Part Coordinates, Actual Nose Cone Scan.**

The turbine blade has a tail with sharp corners, which enabled us to demonstrate the ability of the adaptive scanning algorithm to detect and navigate corners. The results for this scan are shown in Figures 13, 14, and 15 below. The internal surface of the blade could not be scanned because of mechanical interference with the mounting bracket of the structured light. This portion of the blade can be easily scanned with a different bracket design.

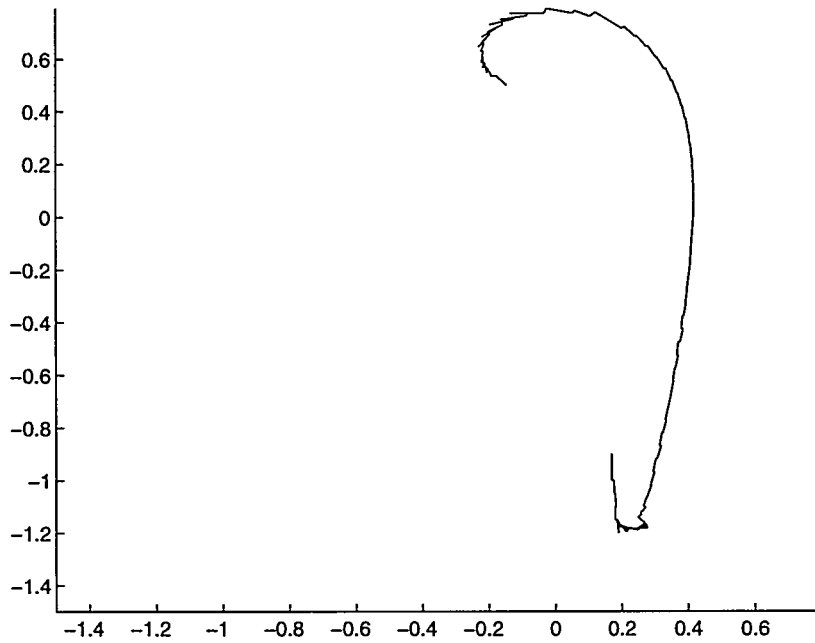


**Figure 13 Path of Point B, in Part Coordinates, Actual Turbine Blade Scan.**

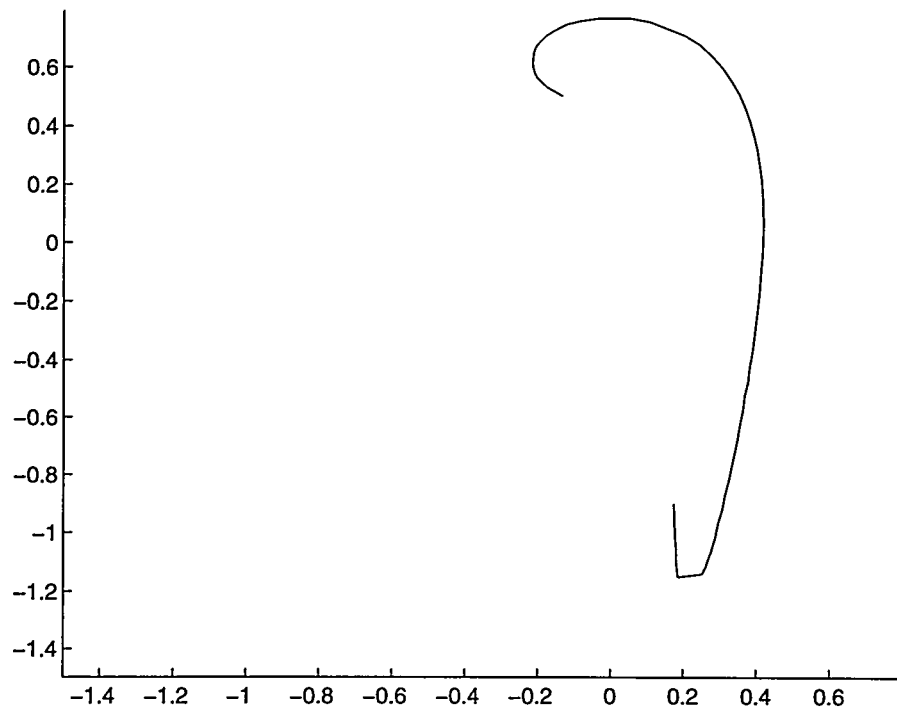


**Figure 14** Path of Point D, in Part Coordinates, Actual Turbine Blade Scan.

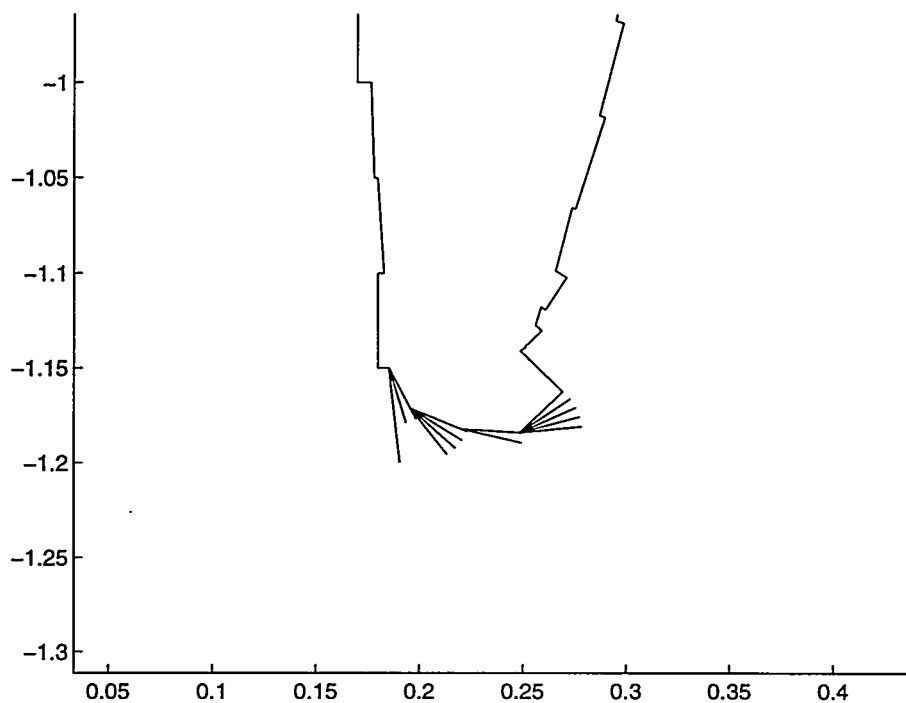


**Figure 15** Path of Point B, in Part Coordinates, Blow-up of Corner Detection/Navigation, Actual Turbine Blade Scan.

## Conclusion

The automatic tool path generation system was found to perform successfully for blades with relatively few flaws and defects. The fuzzified lowess digital filter allows the tool path generation system to function properly for blades with burrs, holes, and overspray. In summary, the fuzzified lowess filter improves the automatic tool path generation process so that:

1. higher resolution scanning data are passed to the surface analysis code which improves the curve fitting and CAD model generating process,
2. the surface normals generated in the CAD file are "filtered" to reduce oscillation of the tool path.

It is expected that these improvements will result in a process that meets the manufacturer's accuracy requirements. Optimization and automation of the individual process steps will be performed to minimize the total cycle time. Also for application to general parts, the adaptive scanning algorithm was developed and successfully scanned a right pyramid and an ellipsoid in simulation studies. In actual experiments, a nose cone and a turbine blade were successfully scanned. A complex shaped turbine blade was successfully scanned and finish machined using these algorithms.

## References

- [1] Zadeh, L.A., "Outline of a New Approach to the Analysis of Complex Systems and Decision Processes," *IEEE Transactions on Systems, Man, and Cybernetics*, vol. SMC-3, no. 1, pp 28-44, 1973.
- [2] Mamdani, E.H. and S. Assilian, "An Experiment in Linguistic Synthesis with a Fuzzy Logic Controller," *Int. J. Man-Machine Studies*, Vol. 7, pp 1-13, 1975.
- [3] Maiers, J. and Y.S. Sherif, "Application of Fuzzy Set Theory," *IEEE Transactions on Systems, Man, and Cybernetics*, vol. SMC-15, no. 1, pp 175-189, 1985.
- [4] Cleveland, W.S., "Robust Locally Weighted Regression and Smoothing Scatterplots," *Journal of the American Statistical Association*, vol. 74, No. 366, Part 2, pp 829-836, 1979.
- [5] Kwok, K.S., Driessen, B.J., and C.S. Loucks, "Automatic Tool-path Generation for Finished Machining," *IEEE International Conference on Robotics and Automation*, Albuquerque, New Mexico, pp 1229-1234, April 1997.

## Appendix A

### Adaptive Scanning Algorithm

Note: "Take scan" always returns  $\alpha$ ,  $\bar{v}_s$ ,  $x_D$ ,  $y_D$ ,  $z_D$ . Note: "Take scan" returns a value of  $\alpha = 10^{10}$  if the scan is unacceptable. Otherwise, it returns the distance between points B and D.

Note: "Rotate about B" means command a physical rotation of the tool vector, while keeping point B fixed (in part coordinates).

Note: "Translate B" means command a physical translation of the scanner (in part coordinates), while keeping the tool vector constant.)

Starting values of  $x_B$ ,  $y_B$ ,  $z_B$ , and  $\bar{n}$  are provided by the user and match the physical current position of the scanner.

Let the initial step direction  $\bar{v}$  be  $-90^\circ$  about the z-axis from the projection of the initial  $\bar{n}$  onto the x-y plane.

Let  $\text{stepmax} = \{0.1"\}$ . Let  $\text{step} = \text{stepmax}$ .  $\text{noise\_level} = \{0.003"\}$ . Let  $\text{step\_corner} = \{10\} * \text{noise\_level}$ . Let  $\text{stepvs\_start} = \{0.1"\}$ .

Let  $\text{step\_total} = 10^{10}$ . Let  $\text{step\_total\_min} = 2\pi(0.25")$ .

While  $\text{step\_total} > \text{step\_total\_min}$

    Let  $\theta = 0$ . Let  $\text{step\_total} = 0$ .

    While  $\theta \leq 2\pi$

        Translate B in  $\bar{v}$  by amount step. Take scan.

        While scan is unacceptable (i.e.,  $\alpha > 10^{10} / 2$ )

$\text{step} = \text{step} / 2$

            Translate B in  $-\bar{v}$  by step. Take scan.

            If  $\text{step} < 3 \text{ noise\_level}$  (corner detected)

                Translate B in  $-\bar{v}$  by amount step

                Let  $\alpha_{\text{old}} = 10^{10}$ . Let  $\alpha = 10^{10}$ .

$\beta = 10^\circ$ .

                While  $\alpha \leq \alpha_{\text{old}}$

$\alpha_{\text{old}} = \alpha$

                    Rotate  $\bar{n}$  by amount  $\beta$  about the z-axis.

                    Rotate about B to align toolvector with  $\bar{n}$ .

                    Let  $\bar{v} = \text{Rot}(z, \beta)^T \bar{v}$  (rotates  $\bar{v}$  about z-axis by amount  $\beta$ .)

                    Translate B in  $\bar{v}$  by amount  $\text{step\_corner}$ .

                    Take scan.

                    if  $\alpha \leq \alpha_{\text{old}}$

                        Translate B in  $-\bar{v}$  by  $\text{step\_corner}$ .

                    Endif

```

        Endwhile
    Endif
    Let  $\bar{v}_{old} = \bar{v}$ 
     $\Delta\theta = caldth(x_D, y_D, x_{Dold}, y_{Dold})$ . (Note: function caldth is defined
    below this algorithm description).
     $\theta = \theta + \Delta\theta$ .
     $\bar{v} = \begin{pmatrix} x_D - x_{Dold} \\ y_D - y_{Dold} \\ 0 \end{pmatrix}$ .  $\bar{v} = \bar{v} / \|\bar{v}\|$ .
    if  $\bar{v}^T \bar{v}_{old} < 0$ 
         $\bar{v} = -\bar{v}$ 
    Endif
    step_total = step_total + step
    step_fuz = step
    step = min(2 step, step_max)
    Let  $x_{Dold} = x_D$ ,  $y_{Dold} = y_D$ ,  $z_{Dold} = z_D$ .
     $\bar{n} = \bar{v} \times \bar{v}_s$ .  $\bar{n} = \bar{n} / \|\bar{n}\|$ 
    if  $\bar{n}^T \bar{n}_{current} < 0$  (where  $\bar{n}_{current}$  is the current tool vector.)
         $\bar{n} = -\bar{n}$ 
    Endif
    Let  $\bar{n}_{fuz} = \begin{pmatrix} n(1) \\ n(2) \end{pmatrix}$ . Let  $\bar{n}_{fuz} = \bar{n}_{fuz} / \|\bar{n}_{fuz}\|$ .
    Let  $\bar{n}_{old,fuz} = \begin{pmatrix} n_{old}(1) \\ n_{old}(2) \end{pmatrix}$ .  $\bar{n}_{fuz,old} = \bar{n}_{fuz,old} / \|\bar{n}_{fuz,old}\|$ .
    Let  $\theta_{fuz} = \max(\left| \cos^{-1}(\bar{n}_{fuz}^T \bar{n}_{fuz,old}) \right|, 10^{-6})$ 
    Let  $r_{fuz} = step\_fuz / \theta_{fuz}$ .
    Fuzzy Rule Set for Step_Size Selection:
        if  $r_{fuz}$  is small, step_fuz is small.
        if  $r_{fuz}$  is medium, step_fuz is medium.
        if  $r_{fuz}$  is large, step_fuz is large.
    step = min(step, step_fuz).
    Let  $\bar{n} = (\bar{n} + \bar{n}_{old}) / 2$ . Let  $\bar{n} = \bar{n} / \|\bar{n}\|$ . (smoothes the toolvector
    trajectory.)
    Let  $\bar{n}_{old} = \bar{n}$ .
    Translate B to place B at  $\begin{pmatrix} x_D \\ y_D \\ z_B \end{pmatrix}$ .
    Rotate about B to align toolvector with  $\bar{n}$ .
EndWhile scan is unacceptable.
(Now we will make a step upward along surface tangent):

```

```

Let step_vs = stepvs_start .
Let  $\alpha = 10^{10}$ . Let  $\bar{v}_{sold} = \bar{v}_s$  .
if  $v_{sold}(3) < 0$ 
     $\bar{v}_{sold} = -\bar{v}_{sold}$  .
Endif
(Now subtract out from  $\bar{v}_{sold}$  the projection of  $\bar{v}_{sold}$  onto  $\bar{v}$ ):
 $\bar{v}_{sold} = \bar{v}_{sold} - \bar{v}_{sold}^T \bar{v}$  .  $\bar{v}_{sold} = \bar{v}_{sold} / \|\bar{v}_{sold}\|$ .
While  $\alpha > 10^{10} / 2$ 
    Translate B in  $\bar{v}_{sold}$  by amount step_vs.
    if  $\alpha > 10^{10} / 2$ 
        Translate B in  $-\bar{v}_{sold}$  by amount step_vs.
        step_vs = step_vs / 2.
    Endif
    Let  $x_{Dold} = x_D$ ,  $y_{Dold} = y_D$ ,  $z_{Dold} = z_D$ .
Endwhile
Endwhile
Endwhile

function caldth:
 $\Delta\theta = \text{caldth}(x_{Dold}, y_{Dold}, x_D, y_D)$ :
    normv =  $(x_{Dold}^2 + y_{Dold}^2)$ 
    normw =  $(x_D^2 + y_D^2)$ 
    if normv > 1e-16
         $\bar{v} = \begin{pmatrix} x_{Dold} \\ y_{Dold} \\ 0 \end{pmatrix} / \sqrt{x_{Dold}^2 + y_{Dold}^2}$ 
    Endif
    if normw > 1e-16
         $\bar{w} = \begin{pmatrix} x_D \\ y_D \\ 0 \end{pmatrix} / \sqrt{x_D^2 + y_D^2}$ 
    Endif
    if normv < 1e-16 or normw < 1e-16
         $\Delta\theta = 0$ 
    else
         $\Delta\theta = |\cos^{-1}(v^T w)|$ 
    Endif

```

## **Distribution**

1	MS-0151	G. Yonas, 9000
1	MS-0188	C.E. Meyers, 4523
1	MS-1002	P.J. Eicker, 9600
20	MS-1003	K.S. Kwok, 9602
5	MS-0439	B.J. Driessen, 9234
5	MS-1006	C.S. Loucks, 9671
1	MS-1003	R.W. Harrigan, 9602
1	MS-1003	R.D. Robinett, 9611
1	MS-1006	P. Garcia, 9671
1	MS-1007	A.T. Jones, 9672
1	MS-1008	J.C. Fahrenholtz, 9621
1	MS-1010	M.E. Olson, 9622
1	MS-1176	R.D. Palmquist, 9651
1	MS-9018	Central Technical Files, 8940-2
5	MS-0899	Technical Library, 4916
2	MS-0619	Review & Approval Desk, 12690 For DOE/OSTI